Generation of Monocycle-Like Optical Pulses Using Induced-Phase Modulation between Two-Color Femtosecond Pulses with Carrier Phase Locking

Mikio Yamashita, Hiroyasu Sone, Ryuji Morita, and Hidemi Shigekawa

Abstract—**Detailed numerical analysis of monocyclical optical pulse generation using induced-phase modulation between two-color carrier-phase-locked femtosecond pulses is presented. For the generation of a short pulse with a quasi-linear chirped white-continuum spectrum, it is found to be important that the large spectral broadening of each input pulse after fiber propagation is as similar as possible and the total spectral intensity of the synthesized wave at the fiber output is as homogenous as possible. As a result, it is shown that a 2.2-fs 1.3-cycle pulse is generated.**

Index Terms—**Induced-phase modulation, monocyclical optical pulse, nonlinear propagation, optical wave synthesis, quasi-linear chirped white-continuum spectrum, spatial phase modulation, two-color carrier-phase-locked femtosecond pulses.**

I. Introduction

In an effort to generate ultrashort optical pulses, many studies have been carried out by a pulse compression technique in which dispersive self-phase modulation (SPM) in a single-mode fiber and chirp compensation with dispersive lines are utilized. In 1987, amplified dye-laser pulses were compressed to 6 fs [1]. Recently, there have been two significant developments based on mode-locked Ti : sapphire laser technology for ultrashort pulse generation. That is, 13-fs 3-MW output pulses from a mode-locked cavity-dumped laser have been compressed to 5 fs using a conventional fused-silica fiber [2]. Furthermore, another group has reported that 20-fs 1-GW near-infrared pulses have been compressed to 4.5 fs using a noble-gas-containing capillary glass fiber [3]. However, for shorter pulse generation, this method utilizing SPM in the capillary fiber with a low nonlinear refractive index n_2 requires high input peak power, and hence has the problem that optical breakdown occurs due to multiphoton ionization and single-mode propagation converts easily to multimode due to self-focusing [3], [4].

On the other hand, recently various methods without utilizing SPM in a fiber have been proposed for ultrashort pulse generation. These include synthesizing optical waves with frequency equidistancy [5], generating phase-controlled high-order harmonic XUV waves [6], and employing the interaction between a free electron beam and a high-power femtosecond optical beams [7]. However, it is difficult to demonstrate these methods experimentally because of the requirements of highly precise techniques and a complex system.

In this paper, we propose another approach using induced-phase modulation (IPM) between two femtosecond pulses with a constant carrier phase difference (hereafter we refer to this approach as the mutual IPM method), instead of SPM. These pulses are generated by the fundamental wave (ω_{01}: the carrier angular frequency of the I_1 pulse) and its second-harmonic (SH) wave ($\omega_{02} = 2\omega_{01}$: the carrier angular frequency of the I_2 pulse) from one common femtosecond pulse of a commercially available Ti : sapphire laser system. In addition, output nonlinear chirp from a short single-mode fiber is compensated for by a spatial phase modulator.

To find the optimum input pulse parameters for monocycle-like pulse generation, detailed computer calculation is carried out. As a result, it is shown that 1.3–1.4 cycle pulses corresponding to 2.2–2.3-fs pulsewidths are generated.

II. System Concept and Analysis

A. System Concept for Monocycle-Like Pulse Generation

In Fig. 1, a schematic of a system concept for the generation of monocycle-like optical pulses is illustrated. In the mutual IPM method for monocyclization, the following points are essential. First, when the SH wave $\omega_{02} = 2\omega_{01}$ (I_2 pulse) is produced using the common fundamental femtosecond wave ω_{01} (I_1 pulse), the carrier phase difference between their waves is kept constant according to an equation $\phi_{02} - \phi_{01} = (2n+1)\pi/2 + \phi_{01}$ where ϕ_{0i} denotes the carrier phase of the I_i pulse ($i = 1$–2; n is an integer) [8]–[11]. This is because the conditions of phase matching and frequency conservation are satisfied to ensure cumulative in-phase addition of the radiation power in the second-order nonlinear processes. This enables us to synthesize constructively two spectrally broadened waves at the fiber output after dispersive IPM and SPM in the short fiber. Second, the mutual IPM is spectrally broadened two times more efficiently than SPM only [12]–[14]. Third, the relative values of input pulse durations between the two pulses and the propagation distance are chosen under the condition

Manuscript received December 15, 1997; revised July 29, 1998.

M. Yamashita and R. Morita are with the Department of Applied Physics, Hokkaido University and CREST, Japan Science and Technology Corporation (JST), Sapporo 060, Japan.

H. Sone is with the Department of Electrical and Electronic Engineering, Muroran Institute of Technology and CREST, Japan Science and Technology Corporation (JST), Muroran 050, Japan.

H. Shigekawa is with the Institute of Materials Science and the Center for Tsukuba Advanced Research Alliance (TARA), University of Tsukuba, and CREST, Japan Science and Technology (JST), Tsukuba 305, Japan.

Publisher Item Identifier S 0018-9197(98)08087-7.

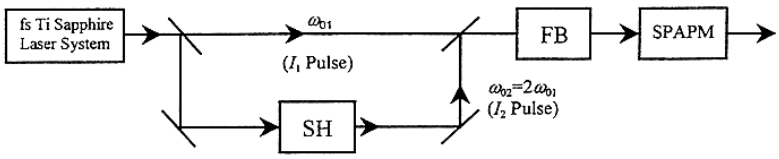

Fig. 1. An experimental system concept for monocyclical pulse generation. SH, FB, and SPAPM denote second-harmonic generation, a short single-mode fiber, and a spatial phase modulator, respectively.

of equal input peak powers between them so that at the fiber output the broadened frequency bandwidth of the deduced spectrum of each pulse becomes almost equal to one another and each pulse spectrum slightly overlaps and interferes with one another at each spectral edge. For the estimation of equal broadening, the ratio of the dispersion length of the I_2 pulse to that for the I_1 pulse is one of the useful parameters. Finally, moderate nonlinear chirp at the fiber output, i.e., the sum of the two linear chirps, is effectively compensated for by a spatial phase modulator [15].

B. Fundamental Equation and Analytical Method

The basic analysis for nonlinear propagation of different color pulses and chirp compensation by spatial phase modulation was described in [16]. We summarize the analytical procedures using similar notation. The coupled equations in the normalized group-velocity coordinate (ξ_1, τ_1) of the I_1 pulse, which describe the nonlinear propagation of the normalized electric field envelopes $u^{(i)}(\xi_1, \tau_1)$ of the two pulses $I_i (i = 1\text{–}2)$ with the normalized parameter T_{0i} of the initial pulse duration $t_{p,i}$, are as follows:

$$\frac{\partial u^{(1)}(\xi_1, \tau_1)}{\partial \xi_1} = -\frac{j}{2}\,\mathrm{sgn}(\ddot{k}_{01})\,\frac{\partial^2 u^{(1)}(\xi_1, \tau_1)}{\partial \tau_1^2} + \beta_{01}\,\frac{\partial^3 u^{(1)}(\xi_1, \tau_1)}{\partial \tau_1^3} + j\left[\left|u^{(1)}(\xi_1, \tau_1)\right|^2 + 2g_{12}\left|u^{(2)}(\xi_1, \tau_1)\right|^2\right]u^{(1)}(\xi_1, \tau_1) \tag{1}$$

$$\frac{\partial u^{(2)}(\xi_1, \tau_1)}{\partial \xi_1} = -\frac{j}{2}\,\mathrm{sgn}(\ddot{k}_{02})S_{12}\,\frac{\partial^2 u^{(2)}(\xi_1, \tau_1)}{\partial \tau_1^2} + S_{22}\,\frac{\partial^3 u^{(2)}(\xi_1, \tau_1)}{\partial \tau_1^3} + S_{32}\,\frac{\partial u^{(2)}(\xi_1, \tau_1)}{\partial \tau_1} + jS_{42}\left[\left|u^{(2)}(\xi_1, \tau_1)\right|^2 + 2g_{21}\left|u^{(1)}(\xi_1, \tau_1)\right|^2\right]u^{(2)}(\xi_1, \tau_1) \tag{2}$$

where $u^{(2)}(\xi_1, \tau_1) \equiv u^{(2)}(a_2\xi_1, b_2\tau_1 + c_2 + d_2\xi_1)$, $b_2 = T_{01}/T_{02}$, $c_2 = -t_{20}/T_{02}$, $d_2 = (\dot{k}_{01} - \dot{k}_{02})T_{01}^2/(T_{02}|\ddot{k}_{01}|)$, $S_{12} = |\ddot{k}_{02}|/|\ddot{k}_{01}|$, $S_{22} = \beta_{02}|\ddot{k}_{02}|T_{02}/|(\ddot{k}_{01}|T_{01})$, $S_{32} = (\dot{k}_{01} - \dot{k}_{02})T_{01}/|\ddot{k}_{01}|$, $a_2 = S_{42} = |\ddot{k}_{02}|T_{01}^2/(|\ddot{k}_{01}|T_{02}^2)$, and $g_{mn} = |\ddot{k}_{on}|\omega_{om}T_{om}^2/[|\ddot{k}_{om}|\omega_{on}T_{on}^2]$. In deriving the equations, the following assumptions were made. The third-order nonlinear polarization terms other than the nonlinear refractive index ones were neglected because their polarizations do not generally contribute significantly under the condition of nonphase-matching in four-wave-mixing processes in single-mode fiber [12]. In addition, two different values of the linear refractive index n_{0i}, wavenumber k_{0i}, the reciprocal of the group velocity $\dot{k}_{0i}$, the group-velocity dispersion (GVD) $\ddot{k}_{0i}$ and the third-order dispersion $\dddot{k}_{0i}$ (β_{0i} is its normalized one) at the carrier angular frequency ω_{0i} of each input pulse I_i are applied as representative values in the ultrabroad-band frequency region $g_{mn} \fallingdotseq 1$. The first and second terms of the equations represent the GVD and the third-order dispersion, respectively, the third term in (2) represents the group-velocity mismatching between the I_1 and I_2 pulses, the third term in (1) and the fourth term in (2) represent SPM, and the fourth term in (1) and the fifth term in (2) represent IPM.

TABLE I
INPUT PULSE AND FIBER PARAMETERS

		1st Pulse I_1		2nd Pulse I_2
		ω_{01}	$\omega_{0c}=3\omega_{01}/2$	$\omega_{02}=2\omega_{01}$
Input Pulse				
	λ_{0i} [nm]	750	500	375
	$t_{p,i}$ [fs]	30~50		42.4~70.7
	P_{0i} [kW]	500~1000		500~1000
	t_{i0} [fs]	0		~-87.7
Fiber				
	n_2 [m^2/V^2]		1.22×10^{-22}	
	d [μm]		2	
	z_0 [mm]		~0.9	
	$\dot{k}$ [s^2/m]	4.036×10^{-26}		10.741×10^{-26}
	$\ddot{k}$ [s^3/m]	2.605×10^{-41}		3.248×10^{-41}

We solve numerically the above coupled equations for a fused-silica fiber with a core diamater of 2 μm and a nonlinear refractive index $n_2 = 1.22 \times 10^{-12}$ (m/V)^2 [17] using the split-step Fourier method [12], under the assumption that the initial pulse shapes $I_i(\tau_i)$ are sech^2 at $\xi_i = 0$. Typical input pulse parameters employed for the calculations are shown in Table I. They are chosen by taking into account the output pulse characteristics obtained from a commercially available Ti : sapphire laser system.

At the fiber output, $z_0 (= (T_{01})^2\xi_{10}/|\ddot{k}_{01}|)$, the amplitude $A_T(z_0, t)$ of the total electric field $E_T(z_0, t) = 2^{-1}A_T(z_0, t)\exp[-j3\omega_{01}t/2]$ + c.c. of the composite wave is described as follows by regarding $\omega_{0c} = (\omega_{02}-\omega_{01})/2+\omega_{01} = 3\omega_{01}/2$ as a carrier angular frequency:

$$A_T(z_0, t) = (n_{01}/n_{0c})^{1/2}A_1(z_0, t)\exp[j(\omega_{01}t/2 + \phi_{T1})] + (n_{02}/n_{0c})^{1/2}A_2(z_0, t - t_{20}) \cdot \exp[j(-\omega_{01}t/2 + \phi_{T2})] \tag{3}$$

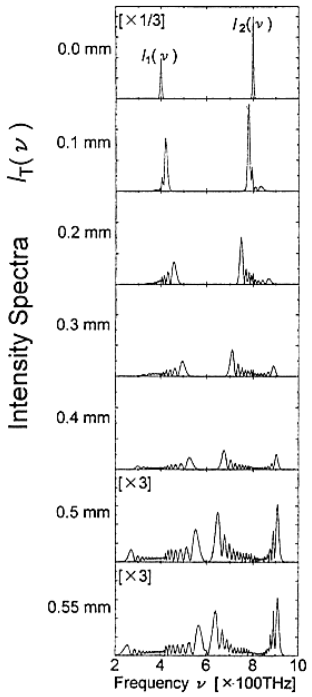

Fig. 2. An example of an evolution of the total intensity spectrum $I_T(\nu)$ during fiber propagation (see the text concerning the values of the parameters).

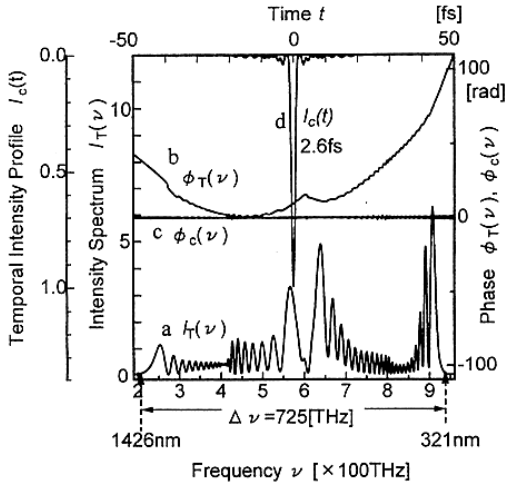

Fig. 3. An example of (a) the total intensity spectrum $I_T(\nu)$, (b) the frequency-dependent phase $\phi_T(\nu)$, (c) the compensated phase $\phi_c(\nu)$, and (d) the compressed pulse $I_c(t)$.

where $A_i(z_0, t - t_{i0}) \equiv (\sqrt{P_{0i}}/N_{sol,i})u^{(i)}(\xi_i, \tau_i)$ is the electric field envelope of the I_i pulse at the fiber output z_0, t_{i0} is the initial delay time of the I_i pulse ($i \neq 1$) relative to the I_1 pulse, P_{oi} is the input peak power, $N_{sol,i}$ is the soliton number, and n_{0c} is the linear refractive index at ω_{0c}. $\phi_{T1} = k_{01}z_0 + \phi_{01}$ and $\phi_{T2} = k_{02}z_0 + \phi_{02} + 2\omega_{01}t_{20}$ which represent the phase constants. The Fourier transform $A_T(\xi_{10}, \Omega) \equiv |A_T(\xi_{10}, \Omega)| \exp[j\phi_T(\xi_{10}, \Omega)]$ of the total envelope $A_T(\xi_{10}, \tau_1)$ at the normalized fiber output distance ξ_{10} in the ξ_1, τ_1 coordinate is obtained from the linear combination of the shifted Fourier transform $U^{(i)}(\xi_{10}, \Omega + \delta_i\omega_{01}T_{10}/2)$ ($\delta_i = -1, 1$ for $i = 1, 2$) of $u^{(i)}(\xi_{10}, \tau_1)$. Consequently, the intensity spectrum $I_T(\Omega)$ and the frequency-dependent phase $\phi_T(\Omega)(\equiv \phi_T(\xi_{10}, \Omega))$ of the fiber output pulse are calculated from $\epsilon_0 c n_{0c}|A_T(\xi_{10}, \Omega)|^2/2$ and $\tan^{-1}(\mathrm{Im}(A_T(\xi_{10}, \Omega))/\mathrm{Re}(A_T(\xi_{10}, \Omega)))$, respectively. Fig. 2 shows an example of the evolution of the intensity spectrum during propagation along the fiber. In addition, Fig. 3 shows an example of the intensity spectrum and the frequency-dependent phase at the fiber output $z_0 = 0.55$ mm, where $P_{01} = P_{02} = 900$ kW, $t_{p,1} = 50$ fs, $t_{p,2} = 70.7$ fs, $\omega_{01} = 2.513 \times 10^{15}$ rad/s ($\lambda_{01} = 750$ nm), $\omega_{02} = 5.027 \times 10^{15}$ rad/s ($\lambda_{02} = 375$ nm), $t_{20} = -53.7$ fs, $\phi_{01} = 0$, and $\phi_{02} = -\pi/2$. From this figure, it is seen that the spectrum is extremely broadened over the near-infrared, the visible, and the near-ultraviolet wavelengths from 320.6 to 1426.4 nm which corresponds to the spectral full width of $\Delta_{\nu T} = 725$ THz. Also, the chirp is moderately nonlinear and is composed of two linear chirps having different slopes.

Next, let us describe chirp compensation by means of a frequency synthesizer utilizing a spatial phase modulator of 256 channels and 12 bits [15]. The full width $\Delta\Omega_T = 2\pi\Delta\nu_T$ of the pulse spectrum is divided by the number of channels so that the frequency-dependent phase component $\phi_T(\Omega_i)(i = 1\text{–}256)$ at the different angular frequencies Ω_i are spatially arrayed with a frequency equidistancy $\Delta\Omega_0 = \Delta\Omega_T/256$. The effect of the gap size between the channels is neglected. The modulator independently controls each channel to give a phase shift $\phi_m(\Omega_i)$ with an accuracy of 12 bits so that the phase difference $\phi_c(\Omega_i) = \phi_T(\Omega_i) - \phi_m(\Omega_i)$ after modulation becomes as small as possible [in practice, $\phi_c(\Omega_i) = \phi_T(\Omega_i) - (2n\pi - \phi_m(\Omega_i))$]. A numerical result for $\phi_c(\Omega_i)$ for the above example is also shown in Fig. 3, which shows that the compensated phase $\phi_c(\Omega_i)$ is kept almost constant. Accordingly, the temporal intensity shape $I_c(\tau_1)$ of the chirp compensated pulse is calculated by the inverse Fourier transform of $|A_T(\xi_{10}, \Omega)| \exp[j\phi_c(\Omega)]$. A result for the example above is also shown in Fig. 3. The FWHM $t_{p,c}$ of the intensity pulse duration of 2.63 fs corresponding to 1.57 cycles for the carrier frequency of $3\omega_{01}/2$ almost agrees with $t_{p,c} = 2.56$ fs for the pulse duration in the case of ideal chirp compensation ($\phi_c(\Omega) = \text{const}$). This result means that the spatial phase modulator is suitable for compensation of nonlinear chirp composed of two different linear chirps.

It was found that the initial phase difference $\phi_{02} - \phi_{01}$ between the I_2 and I_1 pulses does not influence the output-pulse intensity and phase spectra ($I_T(\Omega)$ and $\Phi_T(\Omega)$), except for the small interference part where the highest frequency edge of the I_1 spectrum and the lowest frequency edge of the I_2 spectrum slightly overlap. Consequently, the small variation is compensated for by a small change of the phase modulation and the compressed pulse duration is not affected by the phase difference. Furthermore, it was confirmed that the addition of the higher order dispersion effect of $d^4k_{0i}(\omega)/dw^4$ and $d^5k_{0i}(\omega)/d\omega^5$ to (1) and (2) also do not influence the calculated results.

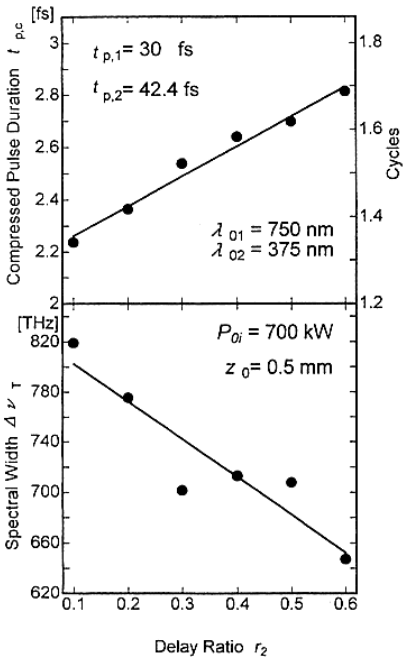

Fig. 4. The typical delay-ratio dependence of the compressed pulse duration $t_{p,c}$ and the total spectral width δD_T for the fiber length $z_0 = 0.5$ mm ($t_{p,1} = 30$ fs, $t_{p,2} = 42.4$ fs, $P_{01} = P_{02} = 700$ kW, $\lambda_{01} = 750$ nm, $\lambda_{02} = 375$ nm).

III. Compressed Pulse Characteristics

To find the optimum input pulse condition, the behavior of the compressed pulse for the different initial delay times t_{20}, peak powers P_{0i}, durations $t_{p,i}$ and fiber length z_0 are investigated in detail.

First, we consider the effect of the initial delay time of the I_2 pulse relative to the I_1 pulse. In the normal GVD region without the nonlinearity of IPM and SPM, in general, the I_2 pulse at the fiber output z_0 is delayed by $z_0(\dot{k}_{01} - \dot{k}_{02})$ relative to the I_1 pulse. Then, for simplification, we introduce a parameter of the delay ratio $r_2 = -t_{20}/[z_0(\dot{k}_{01} - \dot{k}_{02})]$ to examine the delay time effect. Fig. 4 shows typical delay-ratio dependences of the compressed pulse duration $t_{p,c}$ and the intensity spectral width $\Delta\nu_T$ for $P_{01} = P_{02} = 700$ kW, $t_{p,1} = 30$ fs, $t_{p,2} = 42.4$ fs, $\lambda_{01} = 750$ nm, $\lambda_{02} = 375$ nm, and $z_0 = 0.5$ mm. The compressed pulse duration becomes longer with increasing r_2 from 0.1 to 0.6, while the spectral width becomes less broadened. In the range of $r_2 < 0.1$ and $r_2 > 0.6$, the large subpulses (when the ratio of the subpulse peak to the main-pulse peak is larger than 0.1) appear and the pulse duration is broadened due to the significantly low intensity of the central frequency parts of the spectrum of the output synthesized wave. This is because the time area of the overlap between the I_1 and I_2 temporal profiles during propagation and hence IPM is not sufficient to get large spectral broadening before the I_1 pulse leaves the I_2 pulse behind for $r_2 < 0.1$, and after both peak intensities of the I_1 and I_2 pulses decrease owing to dispersive SPM for $r_2 > 0.6$. The r_2-dependence of the spectral broadening of the I_1 pulse is different from that for the I_2 pulse. The spectral width of the latter increases and then decreases more rapidly than that of the former with the increase of the r_2. This is based on the fact that the latter GVD and hence dispersive IPM and SPM are larger than those of the former.

TABLE II
Typical Results of Compressed Pulses at the Optimum Delay Ratio r_2 and Fiber Length z_0 for $\lambda_{01} = 750$ nm and $\lambda_{02} = 375$ nm (See the Text Concerning the Notations)

Input Pulse Duration and Power					Compressed Pulse			
$t_{p,1}$ [fs]	$t_{p,2}$ [fs]	P_{0i} [kW]	z_0 [mm]	r_2	$t_{p,c}$ [fs]	[cycles]	$\eta_c(=t_{p,1}/t_{p,c})$	$\Delta\nu_T$ [THz]
		500	0.90	0.5	2.60	1.56	11.5	714
		600	0.50	0.2	2.41	1.44	12.5	723
30	42.4	700	0.50	0.1	2.24	1.34	13.4	819
		800	0.31	0.2	2.26	1.35	13.3	752
		900	0.23	0.3	2.30	1.37	13.1	742
		1000	0.19	0.4	2.35	1.41	12.8	733
		500	0.90	0.3	2.70	1.62	18.6	623
		600	0.70	0.2	2.53	1.51	19.8	682
50	70.7	700	0.60	0.2	2.43	1.45	20.6	716
		800	0.51	0.2	2.37	1.42	21.1	736
		900	0.43	0.2	2.32	1.39	21.6	747
		1000	0.35	0.3	2.36	1.41	21.2	741

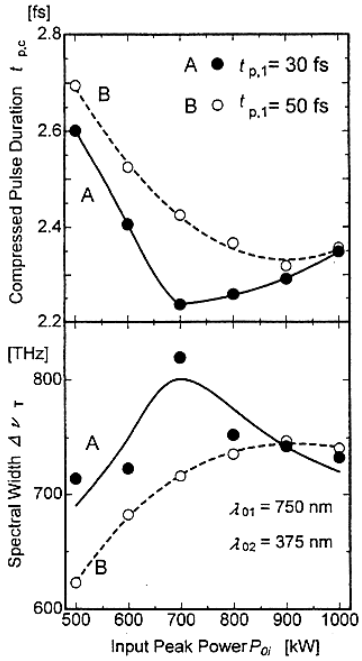

Fig. 5. Input peak power dependence of the compressed pulse duration $t_{p,c}$ and the total spectral width δD_T at the optimum delay ratio and fiber length for the combination of the shorter input-pulse durations [(A) $t_{p,1} = 30.0$ fs, $t_{p,2} = 42.4$ fs] and the combination of the longer ones [(B); $t_{p,1} = 50$ fs, $t_{p,2} = 70.7$ fs] for $\lambda_{01} = 750$ nm and $\lambda_{02} = 375$ nm.

Next, let us discuss how the input peak power and pulse duration affect the compressed pulse. Fig. 5 shows the dependencies of the compressed pulse duration and spectral width on the input peak power $P_{01} = P_{02}$ at the optimum delay ratio and fiber length as a parameter of two different combinations of input pulse durations ($t_{p,1} = 30$ fs, $t_{p,2} = 42.4$ fs, case A, and $t_{p,1} = 50$ fs, $t_{p,2} = 70.7$ fs, case B) for

$P_{01} = P_{02} = 500$–1000 kW, $\lambda_{01} = 750$ nm, and $\lambda_{02} = 375$ nm. The results are summarized in Table II. In case A, the shortest pulse of $t_{p,c} = 2.24$ fs corresponding to 1.34 cycles ($\Delta\nu_T = 819$ THz) is generated at $P_{01} = P_{02} = 700$ kW, $t_{20} = -10.6$ fs, and $z_0 = 0.5$ mm. Around the smaller input power ($\sim$500 kW), the intensity spectral shape becomes more split-like because of the longer propagation distance and hence the more dispersive phase modulation. This results in a longer compressed pulse with larger subpulses. On the other hand, around the higher input power ($\sim$1000 kW), both the deduced I_1 and I_2 spectra broaden asymmetrically because of more rapid up-chirping. Accordingly, the total spectral width becomes a little narrower and the compressed pulse duration becomes a little wider.

These results imply that not only the large spectral broadening but also the intensity homogeneity of the output spectrum and the similarity of the broadened spectral-shape of each pulse are important for the generation of ultrashort pulses.

IV. Conclusion

Optical pulse monocyclization by an IPM + SPM method using two-color carrier-phase-locked femtosecond pulses has been analyzed numerically in detail. As a result, it has been found that a 2.24-fs 1.34-cycle pulse is generated by means of nonlinearly interactive propagation in a 0.5-mm fiber between a 30-fs 750-nm pulse (I_1) and its frequency-doubled 42.4-fs pulse (I_2) with equal power of 700 kW.

This technique for generation of quasi-linear chirped white-spectral pulses can be applied for realization of independently synthesized, multicolor femtosecond beams which are synchronized, as a new optical source such as a femtosecond photon factory. In addition, this technique can be extended to a gas-containing capillary glass fiber for high-power monocyclic pulse generation.

References

[1] R. L. Fock, C. H. Brito Cruz, P. C. Becker, and C. V. Shank, "Compression of optical pulses to six femtoseconds by using cubic phase compensation," *Opt. Lett.*, vol. 12, pp. 483–485, 1987.

[2] A. Baltuška, Z. Wei, U. S. Pshenichnikov, and D. A. Wiersma, "Optical pulse compression to 5 fs at a 1 MHz repetition rate," *Opt. Lett.*, vol. 22, pp. 102–104, 1997.

[3] M. Nisoli, S. de Silvestri, O. Svelto, R. Szipöcs, K. Ferencz, C. Spielmann, S. Sartania, and F. Krausz, "Compression of high-energy laser pulses below 5 fs," *Opt. Lett.*, vol. 22, pp. 522–524, 1997.

[4] M. Nisoli, S. Stagira, S. de Silvestri, O. Svelto, S. Sartania, Z. Cheng, M. Lenzner, Ch. Spielman, and F. Krausz, "A novel-high energy pulse compression system: Generation of multigigawatt sub-5-fs pulses," *Appl. Phys. B*, vol. 65, pp. 189–196, 1997.

[5] T. W. Hänsch, "A proposed sub-femtosecond pulse synthesizer using separate phase-locked laser oscillators," *Opt. Commun.*, vol. 80, pp. 71–75, 1990.

[6] P. B. Corkum, N. H. Burnett, and M. Y. Ivanov, "Subfemtosecond pulses," *Opt. Lett.*, vol. 19, pp. 1870–1872, 1994.

[7] A. C. Melissinos, "QED at 10^{20} W/cm^2," in *Ultrafast Phenomena VIII*. Berlin, Germany: Springer-Verlag, 1993, pp. 34–40.

[8] J. A. Armstrong, N. Bloembergen, J. Ducuing, and P. S. Pershan, "Interactions between light waves in a nonlinear dielectric," *Phys. Rev.*, vol. 127, pp. 1918–1939, 1962.

[9] G. D. Boyd and D. A. Kleinman, "Parametric interaction of focussed Gaussian light beams," *J. Appl. Phys.*, vol. 39, pp. 3597–3639, 1968.

[10] A. Yariv, *Optical Electronics*. Philadelphia, PA: Saunders, 1991, pp. 285–308.

[11] R. Wynands, O. Coste, C. Rembe, and D. Meschede, "How accurate is optical second-harmonic generation?," *Opt. Lett.*, vol. 20, pp. 1095–1097, 1995.

[12] G. P. Agrawal, *Nonlinear Fiber Optics*. San Diego, CA: Academic, 1989, pp. 44–48, 172–179.

[13] M. Yamashita and K. Torizuka, "Numerical study on femtosecond pulse compression by induced phase modulation with group-velocity dispersion effects," *Jpn. J. Appl. Phys.*, vol. 29, pp. 294–298, 1990.

[14] M. Yamashita, K. Torizuka, and T. Uemiya, "Observation of induced phase modulation of femtosecond pulses in glass and organic fibers," in *Ultrafast Phenomena VII*. Berlin, Germany: Springer-Verlag, 1990, pp. 193–195.

[15] A. M. Weiner, D. E. Leaird, J. S. Patel, and J. R. Wullert, "Programmable shaping of femtosecond optical pulses by use of 128-element liquid crystal phase modulator," *IEEE. J. Quantum Electron.*, vol. 28, pp. 908–919, 1992.

[16] M. Yamashita, H. Sone, and R. Morita, "Proposal for generation of a coherent pulse ultra-broadened from near-infrared to near-ultraviolet and its monocyclization," *Jpn. J. Appl. Phys.*, vol. 35, pp. L1194–L1197, 1996.

[17] W. J. Tomlinson, R. H. Stolen, and C. V. Shank, "Compression of optical pulses chirped by self-phase modulation in fibers," *J. Opt. Soc. Amer. B*, vol. 1, pp. 139–149, 1984.

Mikio Yamashita, photograph and biography not available at the time of publication.

Hiroyasu Sone, photograph and biography not available at the time of publication.

Ryuji Morita, photograph and biography not available at the time of publication.

Hidemi Shigekawa, photograph and biography not available at the time of publication.